Nanomed Res J 9(3):274-282, Summer 2024

RESEARCH ARTICLE

$BiFeO_3$@BSA-Gd_2O_3 Nanoparticles as Contrast Agent for Dual Imaging

Zohreh Joorabchi Bokharaei[1], Elham Askarizadeh[2*], Mehdi Khoobi[3], Majid Karimi[4], Ali Masjedi[2]

[1] Department of pharmaceutics, Tehran Azad University of Medical Sciences, Islamic Azad University, Tehran, Iran

[2] Department of Applied Chemistry, Faculty of Pharmaceutical Chemistry, Tehran Azad University of Medical Sciences, Islamic Azad University, Tehran, Iran

[3] Faculty of Pharmacy, Tehran University of Medical Sciences, Tehran, Iran

[4] Polymerization Engineering Department, Iran Polymer and Petrochemical Institute (IPPI), Tehran, Iran

ARTICLE INFO

Article History:
Received 15 Apr 2024
Accepted 08 Jul 2024
Published 01 Aug 2024

Keywords:
$BiFeO_3$
BSA-Gd_2O_3 nanoparticles
CT
MRI
Dual imaging contrast

ABSTRACT

Developing nanoparticles with multimodal contrast agents with therapeutic and contrast effects can greatly improve disease diagnosis. Magnetic resonance imaging (MRI) and computed tomography (CT) are sophisticated medical imaging modalities utilized for visualizing internal tissues and bones, facilitating the diagnosis of organ-related ailments and diseases. In MRI, bovine serum albumin (BSA) is a well-known compound used to carry gadolinium oxide as a contrast agent. Bismuth ferrite nanoparticles ($BiFeO_3$ NPs) have been identified as a novel multifunctional therapeutic agent suitable for applications in radiotherapy, MRI, CT, and as mediators for magnetic hyperthermia. This study presents new NPs that can serve as dual imaging contrast agents for MRI and CT. These novel nanoparticles ($BiFeO_3$@BSA-Gd_2O_3) consist of $BiFeO_3$ nanoparticles, with BSA acting as a carrier for gadolinium oxide nanoparticles. $BiFeO_3$ was synthesized by the sol-gel method and covered with a BSA layer, then gadolinium oxide was added to the BSA layer. Synthesized nanoparticles were identified using different physicochemical methods. The Inductively Coupled Plasma Spectroscopy (ICP) confirms the existence of Gd, Bi, and Fe in the nanoparticle and the average size of nanoparticles regarding to SEM was 120 nm. The presence of $BiFeO_3$ nanoparticles as a promising agent with multi-functional properties such as CT and MRI imaging and BSA-Gd_2O_3 as an MRI contrast agent, the newly synthesized nanoparticle has the potential to be used as nanomedicine for simultaneous MRI and CT as a Dual imaging contrast.

How to cite this article
Joorabchi Bokharaei Z., Askarizadeh E., Khoobi M., Karimi M.,Masjedi A.. $BiFeO_3$@BSA-Gd_2O_3 Nanoparticles as Contrast Agent for Dual Imaging. Nanomed Res J, 2024; 9(3): 274-282. DOI: 10.22034/nmrj.2024.03.005

INTRODUCTION

Nanomedicines have recently gained significant attention, particularly in cancer treatment, where precise tumor localization is crucial. Various methods are used to diagnose capture images and administer the correct drug dosage to patients. One common method is to employ MRI for diagnosing medical conditions, such as tumor lesions and diseases of the brain and spine, without exposing patients to harmful radiation. MRI contrast is typically produced by influencing the relaxation of water protons and can be enhanced by adding contrast agent material. These agents contain paramagnetic metal ions and are evaluated based on their ability to increase the relaxation coefficient of nearby water protons in a concentration-dependent manner. Gadolinium ion (Gd^{3+}) is well-suited for proton relaxation and is the most commonly used metal for this purpose [1]. Gadolinium-based contrast agents have proven to be highly effective in clinical settings, providing essential diagnostic information that is often unattainable with other noninvasive techniques. It is important to note

* Corresponding Author Email: *elhamaskarizadeh@gmail.com*

that free Gd^{3+} is highly toxic and must be used in its stable form to prevent the release of metal ions inside the body[2]. The binding of organic and biological molecules, including proteins, enzymes, antigens, liposomes, DNA, and RNA, is crucial in preventing the release of gadolinium ions within the body [3][4][5][6]. The first gadolinium contrast agent, a complex of Gadolinium with diethylenetriaminepentaacetate (Gd-DTPA), was approved for use in clinical MRI in 1988[7]. Since then, various gadolinium contrast agents have been developed and used for over 25 years, benefiting over 300 million patients worldwide[8]. One of the remarkable compounds in this field is serum albumin, an important plasma protein with multiple physiological functions[9]. Bovine serum albumin has been widely investigated due to its similarity in structure and sequence to human serum albumin. It has potential medical applications, particularly as a biocompatible coating for magnetic nanoparticles[10]. Preserving the natural structure of albumin immobilized on the nanoparticle surface promotes compatibility, prolongs blood circulation, and prevents the undesirable absorption of other proteins[11]. Numerous studies have examined BSA as a carrier compound for gadolinium oxide in MRI as a contrast agent. These studies indicate that nanoparticles modified with BSA and containing gadolinium oxide have been identified as an effective T1 contrast agent for MRI. [12][13][14]. Research has shown that small molecular weight substances that bind to serum albumin easily pass through the vessel wall.

CT is frequently utilized in medical imaging. In certain medical procedures, contrast enhancement is necessary, and iodine-based contrast agents are commonly employed for this purpose. However, due to environmental concerns and other clinical issue, researchers are exploring alternative contrast agents to replace iodine-based ones[15]. Metal nanoparticles exhibit promise for application as CT contrast agents due to their high X-ray attenuation and density. Among the studied nanoparticles are bismuth nanoparticles as potential substitutes for traditional iodine contrast agents. These nanoparticles have a high atomic number (Z:83), which gives them high photoelectric absorption and low toxicity, making them promising materials for use in radiotherapy[16]. Dual imaging, utilizing both CT and MRI, enhances the probability of achieving an accurate diagnosis. MRI is adept at producing high-quality images of soft tissue, while CT imaging offers detailed three-dimensional bone information. Using multiple imaging modalities, such as MRI and CT, can enhance biological diagnosis, resulting in higher sensitivity and penetration. Therefore, combining MRI and CT can produce more accurate diagnostic results compared to using a single imaging modality. As a result, scientists have developed new contrast agents with multimodal imaging capabilities, which are of significant importance. Previous studies have assessed the T_2 contrast capability of $BiFeO_3$ NPs and demonstrated a decrease in T_2 spin relaxation. The relaxation parameter and Hounsfield units were calculated to assess the nanoparticles' effectiveness as a contrast material in MRI. $BiFeO_3$ NPs resulted in brighter CT images and have been approved for contrast enhancement due to their efficacy. Also, $BiFeO_3$ NPs demonstrated minimal cytotoxicity on cell viability, even at high concentrations, indicating excellent in vitro biocompatibility. Intravascular contrast agents stay in the bloodstream longer, allowing for high-resolution magnetic resonance angiography that isn't achievable with typical extracellular fluid agents and $BiFeO_3$ nanoparticles was introduced as a multifunctional theragnostic agent for radiotherapy, MRI, and CT with unique properties for cancer therapy[17]. Extensive studies have been conducted on nanoparticles having bismuth, iron, gadolinium, and gold ions, functionalized with organic compounds to reduce the toxicity of metal nanoparticles, increase biocompatibility, and show MRI/CT dual imaging properties[18] [19][20]. Decorating nanoparticles with functional groups provides them with targeting properties, allowing them to target specific organs and tissues. This process provides dual and multimodal properties to nanoparticles, allowing them to have both diagnostic and therapeutic capabilities. The implementation of this approach ultimately leads to a reduction in treatment-related side effects and a decrease in the overall cost[18] [19].

The purpose of this study is to synthesize bismuth ferrite nanoparticles that are coated with BSA incorporated by Gadolinium oxide for dual imaging applications. Bovine serum albumin, which contains active chemical groups like carboxyl and thiol groups, can interact with gadolinium oxide nanoparticles and bind to bismuth ferrite nanoparticles. The resulting nanoparticle can be used for both MRI and CT scan imaging due to the presence of bismuth ferrite and gadolinium oxide.

The $BiFeO_3$ nanoparticles were synthesized by sol-gel method and functionalized by BSA and Gd_2O_3 nanoparticles were embedded on BSA (scheme 1). The structure of $BiFeO_3$@BSA-Gd_2O_3 nanoparticles was examined using different techniques such as Fourier-transform infrared spectroscopy (FT-IR), Transmission Electron Microscopy (TEM), X-ray diffraction (XRD), Field Emission Scanning Electron Microscopy (FESEM), Energy-Dispersive-X-ray (EDX) mapping analysis, dynamic light scattering (DLS), and Inductively Coupled Plasma (ICP) Spectroscopy.

MATERIALS AND METHODS

The chemicals used in the experiment were sourced from Sigma-Aldrich without any additional purification. The FESEM analysis was carried out using a Zeiss Model SIGMA VP equipped with an EDX elemental map. For TEM analysis, a Zeiss Model EM10C-100KV was used. The FT-IR data was collected using a Thermo Nicolet Nexus 870 Fourier-Transform infrared spectrometer (USA). XRD analysis was performed using a Rigaku Ultima IV X-ray diffractometer with Copper K-Alpha (Cu Kα) radiation (k=0.154 nm). ICP spectroscopy was conducted using the Varian ICP-OES 730-ES instrument. The average MNP particle size (hydrodynamic size) was determined by DLS using a Nanoparticle size analyzer, Scatter scope I.

Synthesis of $BiFeO_3$

In the synthesis of $BiFeO_3$ nanoparticles, the sol-gel method as referenced in [21] was employed. Initially, a clear solution was obtained by dissolving bismuth nitrate ($Bi(NO_3)_3.5H_2O$) and iron nitrate ($Fe(NO_3)_3.9H_2O$) in a 1:1 molar ratio in 20 mL of 20% v/v nitric acid. Then Ethylenediaminetetraacetic acid (EDTA) was added to the above solution as a chemical linker with the same molar ratio concerning metal nitrates. This solution was stirred and heated at 130°C to evaporate all the liquid until the dried gel was obtained. Then the brown powder was subjected to calcinated at 450°C with a ramp rate of 5 °C/min for 2-3 h to produce $BiFeO_3$ nanoparticles.

Hydroxylation of $BiFeO_3$ nanoparticles ($BiFeO_3$-OH)

$BiFeO_3$ NPs (500 mg) was sonicated in aqueous hydrogen peroxide (30 mL, 30 wt. %) and refluxed at 100 °C for 4 hours under vigorous stirring. After centrifugation, residual particles were washed with deionized water three times and placed in a vacuum oven at 80°C for 12 hours[16].

Synthesis of $BiFeO_3$@BSA

$BiFeO_3$-OH nanoparticle (100 mg) was dispersed in 50 mL of 7.4 phosphate buffer and sonicated for half an hour. Then citric acid (500 mg) was dissolved in deionized water (2 mL) and added dropwise to the $BiFeO_3$-OH solution under vigorous stirring at 90°C for 90 min. Finally, to remove excess citric acid, this compound was centrifuged at 12000 rpm and washed 4 times with deionized water[22]. To prepare $BiFeO_3$@BSA nanoparticles, three different ratios of BSA to $BiFeO_3$: 1.2/1, 1/1, and 0.6/1 were considered. With regards to results, further studies were carried out using 0.6/1 ratio. BSA (60mg) and 1-ethyl-3-(3-dimethylaminepropyl)carbodiimide hydrochloride (EDC) (80mg) were dissolved in phosphate buffer (50 mL). Then, $BiFeO_3$-OH (100mg) was dispersed in deionized water (6 mL) and EDC (2mg) was added and stirred. After 6 h, the BSA solution was added dropwise to the $BiFeO_3$-OH solution at 20°C under a mechanical stirrer for 24 h. The $BiFeO_3$@BSA nanoparticles were centrifuged 4 times at 12,000 rpm to remove any unreacted BSAs and $BiFeO_3$@BSA nanoparticles were dried at room temperature under vacuum[23].

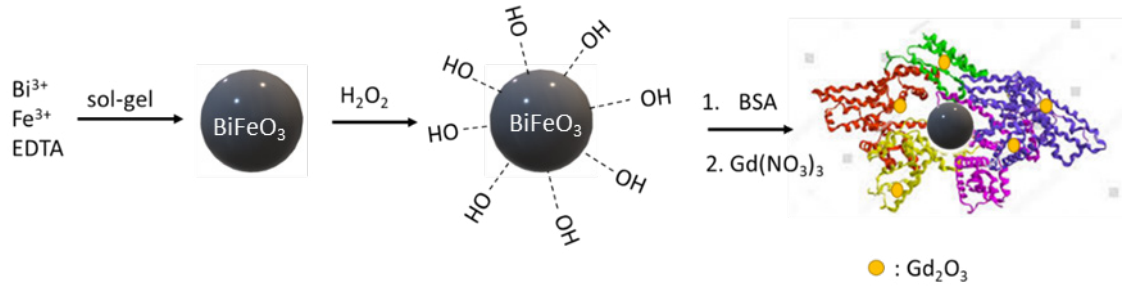

Scheme 1. Representation of synthesis of $BiFeO_3$@BSA-Gd_2O_3 nanoparticle

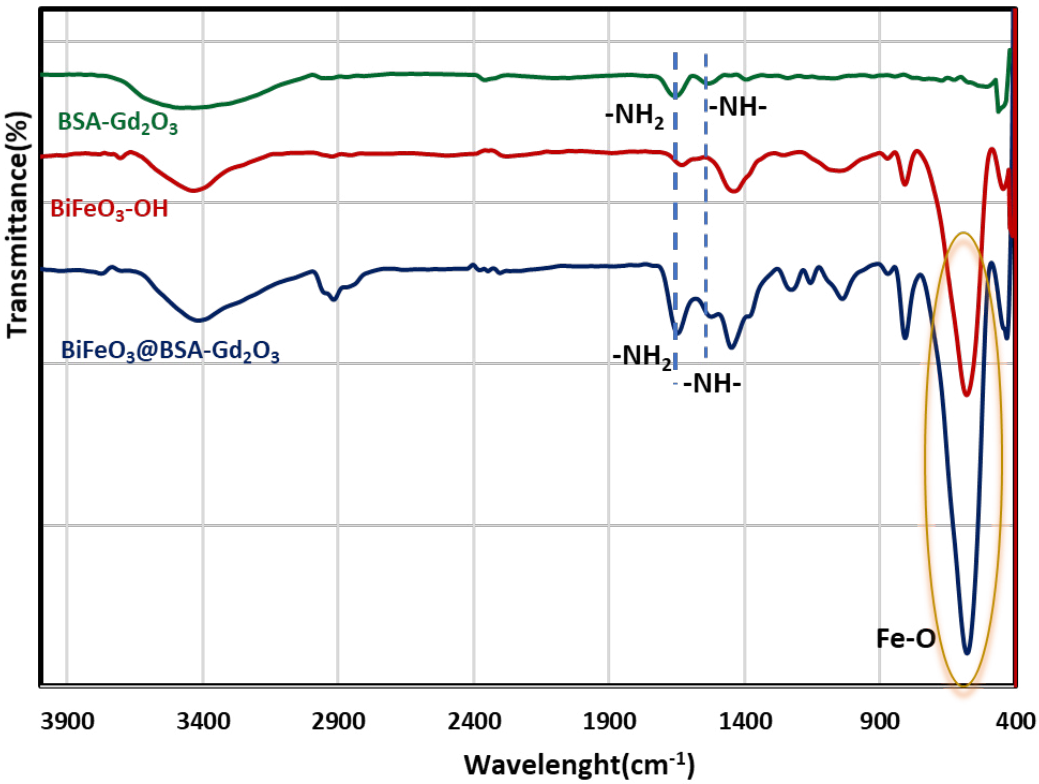

Fig. 1. IR spectra of BSA-Gd_2O_3, $BiFeO_3$-OH, and $BiFeO_3$@BSA-Gd_2O_3

Synthesis of $BiFeO_3$@BSA-Gd_2O_3 nanoparticles

The specified amount of $BiFeO_3$@BSA (100 mg) was dispersed in 20 mL of deionized water for 30 min. Following this, 1 mL of 2 M NaOH was introduced to the mixture and vigorously rotated for 5 min at room temperature. Subsequently, 4.5 mg of gadolinium nitrate was dissolved in 1 mL of deionized water and added dropwise to the BiFeO3@BSA solution, which was then stirred for 12 hours. The resulting mixture underwent centrifugation, followed by three times washes with deionized water and filtration through a 0.22µm microfilter to yield nanoparticles with a size of less than 250 nm [24].

RESULTS AND DISCUSSION

Various physicochemical methods including FT-IR, ICP, XRD, FESEM, DLS, EDX, EDS mapping, and TEM were used to analyze and confirm the synthesis of nanoparticles.

IR spectra of nanoparticles

The infrared spectra of BSA-Gd_2O_3 and $BiFeO_3$-OH, as well as the $BiFeO_3$@BSA-Gd_2O_3 samples, have been studied, and the spectra are presented in Fig. 1. o the stretching vibration of hydroxy groups. Additionally, the peaks seen at 1621 cm^{-1} and 1432 cm^{-1} relate to carboxylic acid groups in EDTA, while the observed. The spectrum of $BiFeO_3$-OH in Fig. 1 displays a broad peak at 3428 cm^{-1}, with the peaks at 451 cm^{-1} and 576 cm^{-1} attributed to the stretching and bending vibrations of the Fe-O group. In the BSA-Gd_2O_3 spectrum, the observed bands at 1644 cm^{-1} and 1523 cm^{-1} are associated with the vibrational bands of amide I (-NH_2) and amide II (-NH-) groups, respectively. The spectrum of $BiFeO_3$@BSA-Gd_2O_3 shows all the characteristic bands related to $BiFeO_3$ and BSA, indicate the stabilizing of BSA on $BiFeO_3$ nanoparticles and the formation of $BiFeO_3$@BSA nanoparticles.

XRD for structural analysis

In Fig, 2. a, the XRD pattern of $BiFeO_3$ nanoparticles is presented, illustrating the phase and crystal structure of the particles. Fig. 2a, indicates that the $BiFeO_3$ NPs are fully crystallized, showcasing differential peaks at 2θ levels of 22.70, 32.11, 37.82, 39.82, 45.89, 51.82, and 56.91 degrees.

These results align with JCPDS reference card number 71-2494, confirming the rhombohedral structure of the BiFeO3 nanoparticle. Some peaks related to impurity Fe_2O_3 and Bi_2O_3 are observed in 2 theta 28° (Bi_2O_3), 32.98° (Fe_2O_3) and 30.5° (Fe_2O_3)[25][26]. Increasing the temperature could lead to pure $BiFeO_3$ nanoparticles[27], but this could potentially remove the functional groups of EDTA, which aid in BSA binding to the surface of $BiFeO_3$ NPs. It's worth noting that these impurities contribute to increased X-ray absorption and the combined magnetic property, which can have a good impact on our composition. After immobilizing BSA-Gd_2O_3 on $BiFeO_3$ nanoparticles, the XRD pattern remained unchanged, indicating that the crystal structure of $BiFeO_3$ did not change after covering by BSA-Gd_2O (Fig, 2. b)

Morphology study of nanoparticles

FESEM images of $BiFeO_3$ and $BiFeO_3$@BSA-Gd_2O_3 were examined to analyze the morphology of nanoparticles and identify chemical compounds. As shown in Fig, 3 (A, B), the $BiFeO_3$ nanoparticles with the average size 120 nm and exhibit a spherical shape. Fig, 3. C shows the $BiFeO_3$@BSA-Gd_2O_3 nanoparticles that besides the spherical nanoparticles, some aggregation can be seen. After passing the nanoparticles through a 0.22µm microfilter, spherical nanoparticles with reduced aggregation were obtained (Fig, 3. D) and passing the filter is crucial to have uniform particles and less aggregation. Fig, 3. (E and F) display the TEM images of $BiFeO_3$@BSA-Gd_2O_3 nanoparticles. The images clearly show that the nanoparticles are semi spherical and have a nearly uniform shape and size. The BSA coats the $BiFeO_3$ nanoparticles, with the dark color representing the $BiFeO_3$ nanoparticles and the light color representing the layer of BSA. Furthermore, the images reveal a core-shell structure with a heterogeneous cover of BSA and some aggregation of $BiFeO_3$ nanoparticles.

The DLS measurement (Fig. 4b) shows that the average hydrodynamic size of $BiFeO_3$@BSA-Gd_2O_3 NPs was measured at 192 nm, a size significantly larger than the values obtained by SEM. The difference in nanoparticle sizes obtained by SEM and DLS is understandable, as SEM provides primary particle diameters of NPs, while the average hydrodynamic diameters obtained by DLS in aqueous suspension include the solvation layer thickness and nanoparticle aggregation. The colloidal stability was evaluated by dispersing $BiFeO_3$@BSA-Gd_2O_3 NPs in deionized water and measuring the hydrodynamic diameter using DLS for 24 hours. After 3 hours, there was a 6-nanometer increase in particle size, followed by no further change for the next 24 hours, as shown in Fig. 4a. The results show that the particles are highly stable with

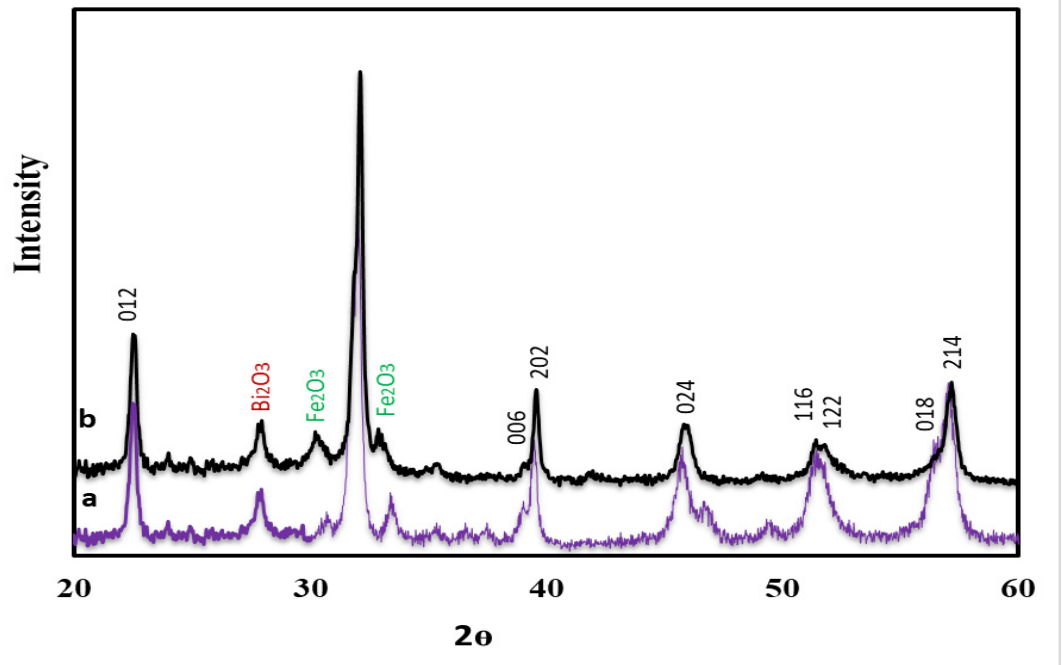

Fig, 2. Diffraction patterns of a: $BiFeO_3$ and b: $BiFeO_3$@BSA-Gd_2O_3

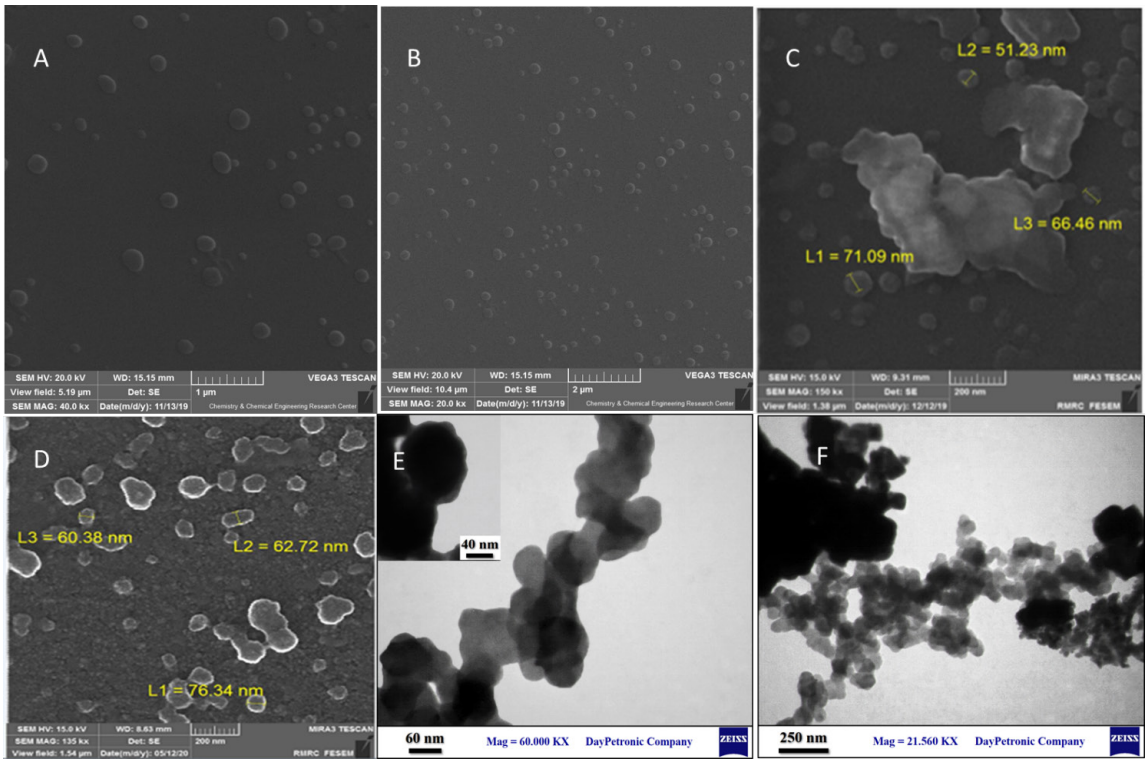

Fig, 3. SEM images A and B: $BiFeO_3$ with different magnifications, C: $BiFeO_3$@BSA-Gd_2O_3 before filtration, D: after filtration, E and F: TEM images of $BiFeO_3$@BSA-Gd_2O_3

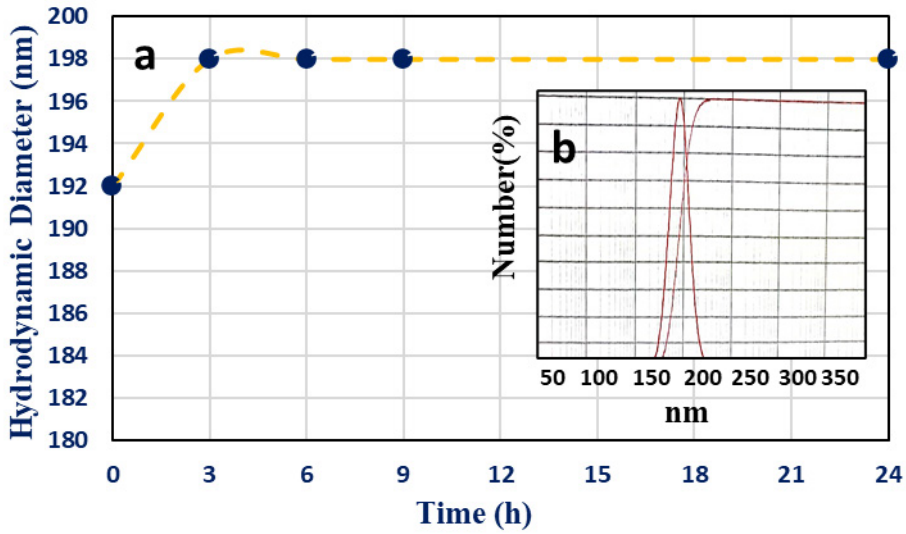

Fig. 4. a: Variation of hydrodynamic diameter of $BiFeO_3$@BSA/Gd_2O_3 with time in deionized water, b: size distribution of $BiFeO_3$@BSA/Gd_2O_3 NPs in deionized water

no aggregation, which supports the idea that BSA-coated NP formulations have enhanced colloidal stability. This is consistent with previous studies that have shown BSA's ability to stabilize nanoparticles [28][29]. These studies also suggest that the size and shape of nanoparticles are important factors in their absorption and performance in the body. The kidneys rapidly excrete nanoparticles smaller than 10 nm, while those larger than 200 nm may trigger the complement system and get removed from the

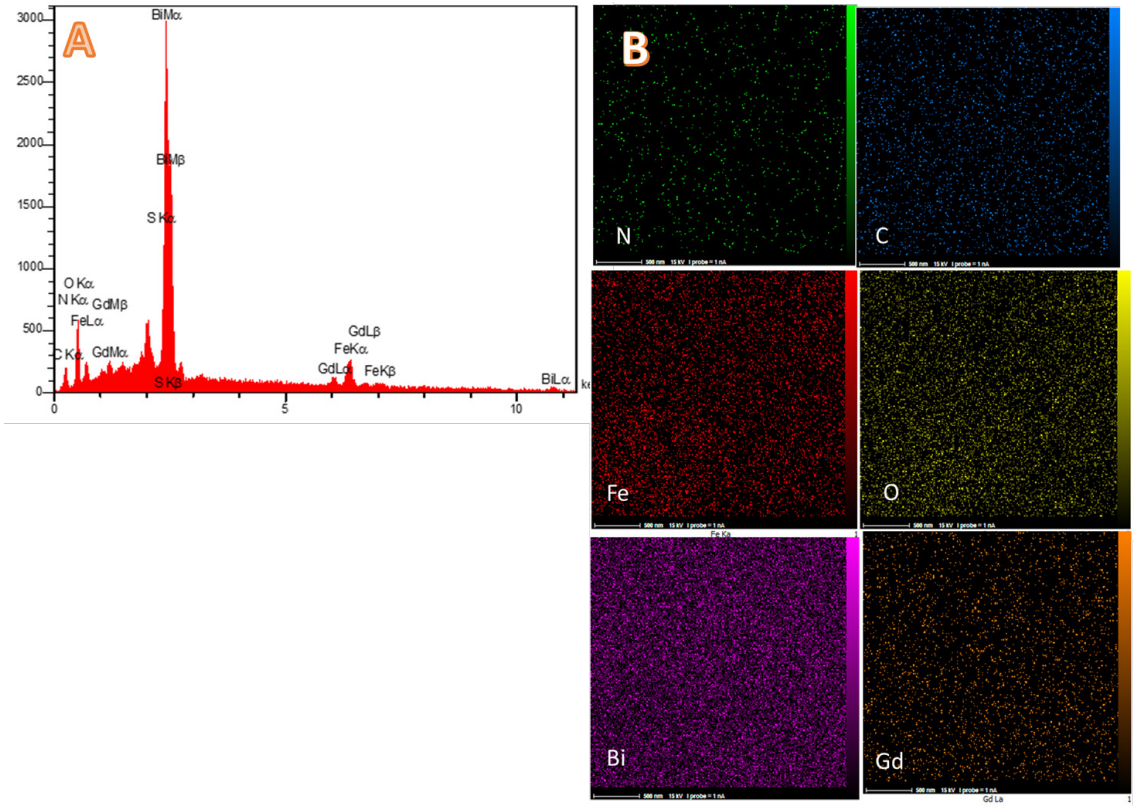

Fig, 5. A: EDS analysis and B: EDX mapping of $BiFeO_3$@BSA-Gd_2O_3

bloodstream quickly [30]. Nanoparticles within the size range of 250 nm to 3 µm have demonstrated optimal in vitro phagocytosis. Moreover, NPs measuring approximately 200 nm preferably utilize alternative uptake pathways, such as clathrin or caveolin-mediated endocytosis. [31]. Based on the results obtained from SEM and DLS, the synthesized nanoparticles with dimensions around 200 nm and without aggregation after 24 hours can be a good candidate for medical applications.

In Fig, 5A, the EDX analysis of $BiFeO_3$@BSA-Gd_2O_3 nanoparticles confirms the presence of Bi, Fe, Gd, O, N, C, and S elements. The elemental mapping pictures are in Fig, 5. B also displays the distribution of Bi, Fe, Gd, O, N, and C elements, indicating that the elements are well distributed and not accumulated in a specific place. The presence of N and S elements indicates the BSA protein layer, while the presence of gadolinium indicates the placement of gadolinium oxide on the BSA surface. In addition, ICP analysis confirms the presence of iron, bismuth, and gadolinium elements in the nanoparticle, and reports the gadolinium percentage as 1.48%.

CONCLUSION

Utilizing dual imaging techniques such as CT and MRI increase the probability of obtaining a more precise and accurate diagnosis. MRI, a non-invasive and robust diagnostic modality in the field of medical science, plays a crucial role in enhancing diagnostic capabilities. Contrast agents are pharmaceuticals that improve the information content of diagnostic images. At present, gadolinium-based complexes are frequently utilized as contrast agents in medical facilities. These agents can speed up longitudinal relaxation (T_1) and generate bright signals. Additionally, magnetic nanoparticles have significant potential for applications in magnetic hyperthermia therapy, enabling clinicians to both diagnose and treat cancer simultaneously. To enhance colloidal stability in biological fluids, gadolinium-based contrast agents are attached to bovine serum albumin. In addition, $BiFeO_3$ nanoparticles are used as the carrier and multifunctional theragnostic agents for radiotherapy and CT scans. In this study, the $BiFeO_3$@BSA-Gd_2O_3 was synthesized as dual imaging contrast for MRI

and CT. $BiFeO_3$ nanoparticles were synthesized and coated with BSA and Gd_2O_3 was coordinated on BSA. The nanoparticles were characterized by FT-IR, FESEM, TEM, Elemental mapping, XRD and ICP techniques. The crystal structures of the nanoparticles were analyzed using XRD, while the morphology was examined using FESEM and TEM. The findings indicated the presence of a BSA coating surrounding the $BiFeO_3$, with an average nanoparticle size of 132 nm. The EDX and ICP techniques confirm the existence of Gd, Bi, and Fe in the nanoparticle. Studies on bismuth ferrite and BSA containing gadolinium ions have shown that the newly synthesized nanoparticle holds significant potential for diagnosing and treating diseases. It can serve as a contrast agent for both MRI and CT scans simultaneously. Based on extensive research regarding the use of $BiFeO_3$ in MRI and CT, as well as BSA as a suitable carrier for gadolinium nanoparticles, and considering the cytotoxic nature of $BiFeO_3$ and BSA, it is evident that the synthesized nanoparticles exhibit significant potential for implementation as a contrast agent in MRI and CT applications. Additionally, DLS and SEM analysis indicate that this compound has an appropriate size for use in nanomedicine applications.

ACKNOWLEDGMENT

The authors acknowledge the support of this study provided by the Tehran Medical Science University, Islamic Azad University, Tehran, Iran.

CONFLICT OF INTEREST

The authors declare that there are no conflicts of interest.

REFERENCES

1. Hao D, Ai T, Goerner F, Hu X, Runge VM, Tweedle M. Review: MR Physics for Clinicians MRI Contrast Agents: Basic Chemistry and Safety. J Magn Reson Imaging. 2012;1071:1060-1071. https://doi.org/10.1002/jmri.23725
2. Coimbra S, et al. Toxicity Mechanisms of Gadolinium and Gadolinium-Based Contrast Agents - A Review. Int J Mol Sci. 2024. https://doi.org/10.3390/ijms25074071
3. Kim H, Lee GH, Chang Y. Gadolinium as an MRI contrast agent. Future Med Chem. 2018. https://doi.org/10.4155/fmc-2017-0215
4. Tetrameric AN, et al. Preclinical Profile of Gadoquatrane. Radiol Imaging. 2022;57(10). https://doi.org/10.1097/RLI.0000000000000889
5. Shaheen RM, Nik NNA, Razak A, Radhi MM, Suardi NB. Comparative bio-effect of gadolinium with alternative contrast medium of magnesium chloride and zinc oxide nanoparticles on single-strand DNA following exposure to magnetic resonance imaging. Iran J Radiat Res. 2024. https://doi.org/10.61186/ijrr.22.1.131
6. Lee W, et al. In vivo evaluation of PEGylated-liposome encapsulating gadolinium complexes for gadolinium neutron capture therapy. Biochem Biophys Res Commun. 2021;568:23-29. https://doi.org/10.1016/j.bbrc.2021.06.045
7. De Hae C, Ph D. Conception of the First Magnetic Resonance Imaging Contrast Agents: A Brief History. Magn Reson Imaging. 2001;12(4):221-230. https://doi.org/10.1097/00002142-200108000-00002
8. Lohrke J, et al. 25 Years of Contrast-Enhanced MRI: Developments, Current Challenges and Future Perspectives. Adv Ther. 2016;33(1):1-28. https://doi.org/10.1007/s12325-015-0275-4
9. Mitin D, et al. Contrast Agents Based on Human Serum Albumin and Nitroxides for 1 H-MRI and Overhauser-Enhanced MRI. Int J Mol Sci. 2024. https://doi.org/10.3390/ijms25074041
10. Chubarov AS. Serum Albumin for Magnetic Nanoparticles Coating. Magnetochemistry. 2022. https://doi.org/10.3390/magnetochemistry8020013
11. M AAP, et al. VEGF-targeted magnetic nanoparticles for MRI visualization of brain tumor. Nanomedicine. 2014. doi: 10.1016/j.nano.2014.12.011. https://doi.org/10.1016/j.nano.2014.12.011
12. You Q, et al. BSA-Bioinspired Gadolinium Hybrids Functionalized Hollow Gold Nanoshells for NIRF/PA/CT/MR Quad-modal Diagnostic Imaging Guided Photothermal/Photodynamic Cancer Therapy. ACS Appl Mater Interfaces. 2017. https://doi.org/10.1021/acsami.7b11926
13. Marasini R. Integration of gadolinium in nanostructure for contrast enhanced-magnetic resonance imaging. Wiley Interdiscip Rev Nanomed Nanobiotechnol. 2019. https://doi.org/10.1002/wnan.1580
14. Xu S, et al. In Situ One-Pot Synthesis of Fe2O3 @ BSA Core-Shell Nanoparticles as Enhanced T1 Weighted Magnetic Resonance Imagine Contrast Agents. ACS Appl Mater Interfaces. 2020. https://doi.org/10.1021/acsami.0c13825
15. Hsu JC, Noël PB, Cormode DP, Sadan T. Nanoparticle contrast agents for X-ray imaging applications. Wiley Interdiscip Rev Nanomed Nanobiotechnol. 2020. https://doi.org/10.1002/wnan.1642
16. Mishra MK, Moharana S, Behera B, Mahaling RN. Surface functionalization of BiFeO3: A pathway for the enhancement of dielectric and electrical properties of poly (methyl methacrylate)-BiFeO3 composite films. J Inorg Organomet Polym Mater. 2017;1-10. https://doi.org/10.1007/s11706-017-0364-1
17. Rajaee A, et al. Multifunctional Bismuth Ferrite Nanoparticles as Magnetic Localized Dose Enhancement in Radiotherapy and Imaging. J Biomed Nanotechnol. 2018;14(6):1159-1168. https://doi.org/10.1166/jbn.2018.2553
18. A new theranostic complex based on bismuth-iron oxide nanoparticle for myocardial ischemia: in vitro study. Theranostics. 2022;7(4):320-329.
19. Abolhasani Zadeh F, Shahhosseini E, Rasoolzadegan S, Özbolat G, Farahbod F. Au nanoparticles in the diagnosis and treatment of ovarian cancer: A new horizon in the personalized medicine. Nanomed Res J, 2022;7(1):1-18. https://doi.org/10.22034/nmrj.2022.01.001
20. Gel dosimetry: The effect of gold nanoparticles on the dose

enhancement in the external radiation therapy. J Radiat Res. 2016;1(1):31-38.
21. Wei J, Xue D. Low-temperature synthesis of BiFeO3 nanoparticles by ethylenediaminetetraacetic acid complexing sol-gel process. Mater Res Bull. 2008;43:3368-3373. https://doi.org/10.1016/j.materresbull.2008.02.009
22. Sahoo Y, et al. Aqueous Ferrofluid of Magnetite Nanoparticles: Fluorescence Labeling and Magnetophoretic Control. J Phys Chem B. 2005;3879-3885. https://doi.org/10.1021/jp045402y
23. Li Z, Qiang L, Zhong S, Wang H, Cui X. Synthesis and characterization of monodisperse magnetic Fe3O4@BSA core-shell nanoparticles. Colloids Surf A Physicochem Eng Asp. 2013;436:1145-1151. https://doi.org/10.1016/j.colsurfa.2013.08.044
24. Li J, et al. Aptamer-Directed Specific Drug Delivery and Magnetic Resonance Imaging of Renal Carcinoma Cells In Vitro and In Vivo. J Biomed Nanotechnol. 2016. https://doi.org/10.1166/jbn.2016.2271
25. Taylor P, Silva J. BiFeO3: A Review on Synthesis, Doping and Crystal Structure. Integr Ferroelectr. 2013;37-41. https://doi.org/10.1080/10584587.2011.574986
26. Vijayanand S, Potdar HS, Joy PA. Origin of high room temperature ferromagnetic moment of nanocrystalline multiferroic BiFeO3. Appl Phys Lett. 2009;182507:9-12. https://doi.org/10.1063/1.313258
27. Mishra MK, Moharana S, Behera B, Mahaling RN. Surface functionalization of BiFeO3: A pathway for the enhancement of dielectric and electrical properties of poly (methyl methacrylate)-BiFeO3 composite films. J Inorg Organomet Polym Mater. 2017. https://doi.org/10.1007/s11706-017-0364-1
28. Ming Yu S, Larmaine A, Roige A. Enhanced stability of superparamagnetic iron oxide nanoparticles in biological media using a pH adjusted-BSA adsorption protocol. J Nanopart Res. 2014;16(7). https://doi.org/10.1007/s11051-014-2484-1
29. Airos A, et al. BSA-coated magnetic nanoparticles for improved therapeutic properties. J Mater Chem B. 2015;3:6239-6247. https://doi.org/10.1039/C5TB00833F
30. Han H. The effect of nanoparticle size on in vivo pharmacokinetics and cellular interaction. Nanomedicine. 2016;11:673-692. https://doi.org/10.2217/nnm.16.5
31. Biswas AK, Islam R, Choudhury ZS. Nanotechnology based approaches in cancer therapeutics. Biomed Mater. 2014. https://doi.org/10.1088/2043-6262/5/4/043001